IGNITION AND COMBUSTION CHARACTERISTICS OF METALLIZED PROPELLANTS

Semi-Annual Report
(June 1989-December 1989)

Prepared by

S. R. Turns, D. C. Mueller, and M. J. Scott

Grant No. NAG 3-1044
C. A. Aukerman
NASA Technical Officer
NASA Lewis Research Center

January 1990

IGNITION AND COMBUSTION CHARACTERISTICS OF METALLIZED PROPELLANTS

Semi-Annual Report

(June 1989-December 1989)

Prepared by

S. R. Turns, D. C. Mueller, and M. J. Scott

Department of Mechanical Engineering
and the
Center for Space Propulsion Engineering
The Pennsylvania State University
University Park, PA 16802

for

NASA Lewis Research Center

Grant No. NAG 3-1044

C. A. Aukerman
NASA Technical Officer

January 1990

SUMMARY

A research program designed to develop a detailed understanding of the secondary atomization and ignition characteristics of aluminum slurry propellants has been initiated. The research focuses on these processes because they are the controlling factors limiting the combustion efficiency of aluminum slurry propellants in rocket applications. A burner and spray rig system allowing the study of individual slurry droplets having diameters from about 10-100 μm was designed and fabricated. The burner generates a near uniform high temperature environment from the merging of 72 small laminar diffusion flames above a honeycomb matrix. This design permits essentially adiabatic operation over a wide range of stoichiometries without danger of flashback. A single-particle sizing system and velocimeter also were designed and assembled. Light scattered from a focused laser beam is related to the particle (droplet) size, while the particle velocity is determined by its transit time through the focal volume. Light from the combustion of aluminum is also sensed to determine if ignition has been achieved. These size and velocity measurements will allow the determination of disruption (microexplosion) and ignition times as functions of droplet sizes and ambient conditions. Components for signal conditioning and data acquisition were defined and fabricated or purchased. Software for data acquisition and processing is presently being developed. Plans for the next six months include the shakedown and calibration of the burner, spray rig, optical systems, and data acquisition systems. Preliminary measurements will be obtained using several aluminum slurry formulations.

TABLE OF CONTENTS

INTRODUCTION

MOTIVATION

The application of slurry or gelled propellants to propulsion has been of interest for several decades. These propellants consist of solid particles suspended in a combustible liquid and can be advantageous because of either energy content per unit mass or per unit volume. Slurries with aluminum, for example, offer a substantial increase in volumetric heat of combustion compared to hydrocarbon fuels [1]. In addition, aluminum is an attractive component because of its ease in handling and because it is nontoxic [2].

For rocket applications, specific impulse and mass density control the payload capability for a fixed vehicle configuration [3]. Thus, high mass density propellant systems, such as Al/RP-1/O_2, become attractive to consider as alternatives to more conventional propellant systems. Additional motivation to study such fuels is their potential for improved safety and liquid rocket controllability. For example, application of metallized propellants to the space shuttle could eliminate the solid rocket boosters. The focus of ongoing studies of metallized propellants at NASA Lewis [2] and the primary focus of this study are on Al/RP-1/O_2 propellant systems. Such propellants are attractive for the reasons given above and represent a realistic starting point for development efforts since a data base already exists for Al/hydrocarbon slurries [4,5].

OBJECTIVES

The overall objective of this study is to develop a fundamental understanding of the ignition and combustion characteristics of aluminum-based slurry propellant droplets. Specific objectives are as follows:

1. The development and application of a burner/spray rig and single-particle optical diagnostics to study the detailed ignition and combustion

behavior of small (10-75 μm) droplets, typical of those encountered in practical applications.

2. Understanding the role of surfactants and gellants (or other additives) in promoting or inhibiting secondary atomization of slurry propellant droplets.

3. The evaluation of the ignition and/or combustion characteristics of new slurry propellant formulations that may result from research by NASA or other contractors.

4. The extension of previously developed analytical models and the development of new models to address the phenomena associated with microexplosions (secondary atomization).

OVERVIEW OF APPROACH

A combination of experiment and analysis is planned to achieve the research objectives. To study small (10-75 μm) slurry droplets, a droplet generator from which a small portion of an atomized spray is extracted will be used in conjunction with a laminar flow, flat-flame burner. Particle sizing and velocity measurements will be accomplished using laser scattering techniques. Detailed descriptions of these systems are presented in subsequent sections of this report. In the analytical effort, models of the ignition and combustion events will be applied by extending our existing models of these processes [4,5] to handle new extremes of droplet sizes and ambient conditions. We also plan to develop a physically realistic numerical model of disruptive ignition phenomena.

PARTICLE SIZING AND VELOCITY DIAGNOSTICS

OPTICAL SYSTEM

Particle size characterization will be accomplished using a single-particle counter technique [6,7]. In particular, the near-forward scatter, two-color, laser light scattering technique of Wang and Hencken [7] provides accurate in situ determination of particle sizes in the range of 10-200 μm, while simultaneously providing a measurement of particle velocity. Schematics of this method of particle sizing and its implementation are shown in Figs. 1 and 2, respectively.

In principle, the two-color laser light scattering technique operates as follows: An Ar-ion laser beam is focused to a waist of approximately 350 μm. The primary signal is generated from light scattered by a particle passing through the focal volume. The magnitude of this signal is related to particle size, with larger particles producing a larger signal. Because the intensity falls rapidly in the edges of the laser beam, only data from particles that pass through the beam's center should be accepted. The He-Ne laser beam is used to indicate the location of a particle within the focal volume. The He-Ne beam is aligned concentrically with the Ar-ion beam, but focused to a much smaller waist of approximately 80 μm. The time-dependent signals associated with scattering of the He-Ne and Ar-ion beams will be compared. Signals that indicate particles passing through the focal volume near the center of the Ar-ion beam will be accepted (cf. Fig. 1). The determination of the particle size will be accomplished by a calibration of the scattered intensity associated with pinholes of known size placed at the focal point.

Since light signals will be recorded as a function of time, analysis will yield time-of-flight for a particle to pass through the focal region. Dividing the Ar-ion beam diameter ($1/e^2$ points) by the time-of-flight will give particle velocity (cf. Fig. 1).

Hardware

All lenses in the optical system are plano-convex lenses made of borosilicate

SINGLE PARTICLE SIZING AND VELOCIMETRY

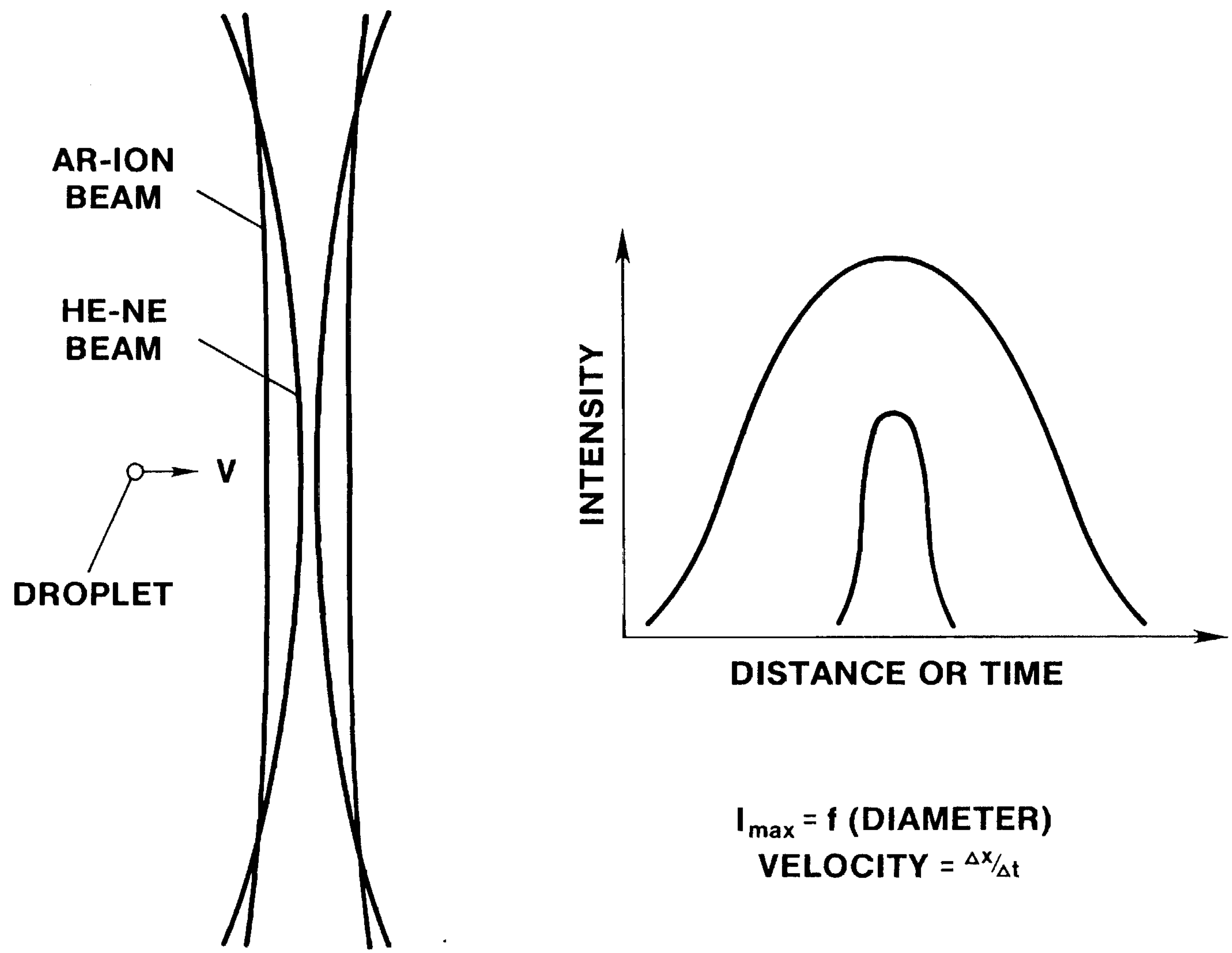

FIGURE 1. Schematic diagram of colinear laser beams with droplet approaching focal volume (left). Also shown (right) are the light intensity profiles of the beams. A particle passing through the center of the focal volume generates a scattered light signal of the same shape.

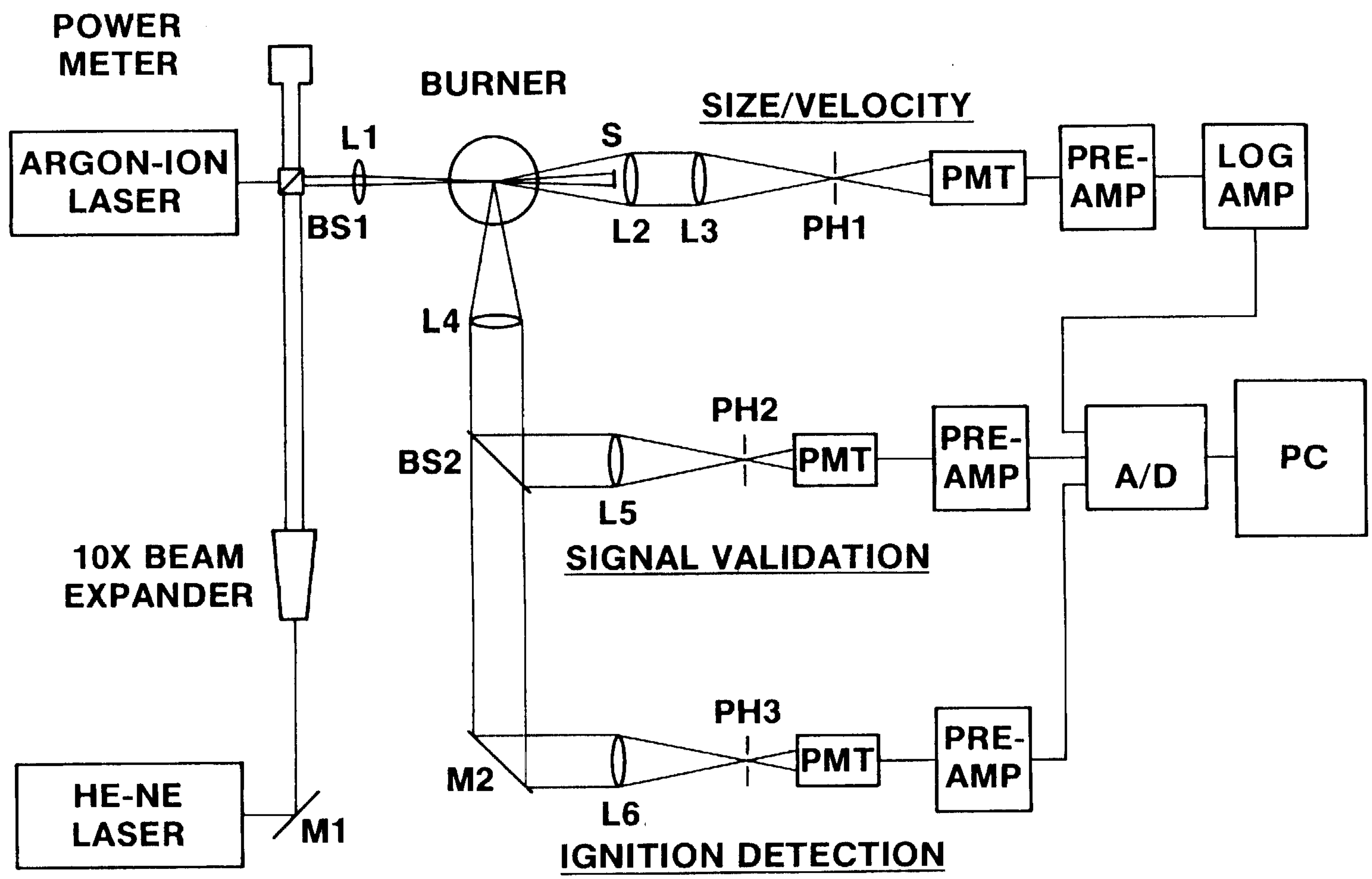

FIGURE 2. Schematic of optical system.

crown glass and manufactured by Oriel. Filters are also manufactured by Oriel. The majority of remaining parts are manufactured by Newport Research Corporation (NRC). Other part manufacturers are noted throughout the text. Information in braces refer to components shown in Fig. 2.

Specifically, the 632.8 nm wavelength light from a He-Ne laser (Spectra-Physics model 124B) is expanded from a beam diameter of 1.1 mm to a beam diameter of 11 mm using a beam collimator (NRC model LC-075). The expanded beam passes through a cube beamsplitter {BS1} (Melles-Griot model 03-BSC-009) where it is concentrically joined with the 488.0 nm wavelength beam from the Ar-ion laser (Lexel model 95). Use of the beamsplitter also permits easy measurement of the laser power for reference. A Lexel model 504 power meter is used as illustrated in Fig. 2. The beams along the primary optical axis are focused through a 750 mm lens {L1} (model 40815), and pass through a light beam chopper (HMS model 230) and an iris (NRC model ID-1.0). The lens focuses the beams to waists of approximately 80 μm for the red He-Ne beam and approximately 350 μm for the blue Ar-ion beam. The particles from the burner pass through the beams at the beam focal location, scattering the light. A 250 mm lens {L2} (model 40790), with a flocking strip across its center to block the direct laser light, receives the near-forward scattered light and collimates it. The collimated light then passes through a second 250 mm lens {L3} to focus it onto a 500 μm pinhole {PH1} (Oriel model 77809). The light then passes through a 488.0 nm filter (model 52630), two 50 mm lens (model 40340) and onto the grid of a photomultiplier tube (Hamamatsu model 1P28A or R928) where the 488.0 nm signal is generated. This signal is used to determine the particle size. The various photomultiplier tubes are powered by either a Pacific Instruments (model 204) or a Power Designs (model 2K20) high-voltage DC power supply.

A second set of receiving optics is located perpendicular to the probe beam optical axis on a line through the focal volume of the sending optics. The 90^{o} scattered light and

the emitted light from an ignited aluminum particle pass through an iris (NRC model ID-1.5) to a 350 mm lens {L4} (model 40800) which collimates the light.

The scattered light is redirected parallel to the near-forward receiving optics by a 50/50 beamsplitter {BS2} (Oriel model 57315). This light passes through a second 350 mm lens {L5} which focuses the light onto a 500 μm pinhole {PH2}. The light passes through a 632.8 nm filter (model 52720), two 50 mm lenses and onto a photomultiplier tube where a signal is generated which is related to the scattering intensity from the red beam.

The emitted light from an ignited aluminum particle passes through an iris (NRC model ID-1.0) to a flat reflector {M2} (Oriel model 44130) where it is redirected parallel to the other receiving channels. This light passes through a second 350 mm lens {L6} and is focused onto a 500 μm pinhole {PH3}. The light then passes through a 440 nm filter (model 53820), two 50 mm lenses, and onto a photomultiplier tube where a signal related to the intensity of emission from an ignited aluminum particle is generated. Comparison of the signal from this channel to the scattered light signals produced at the other two channels will indicate if the particle of interest is ignited.

Calibration Procedure

Calibration of the system is a three-step process. Step one involves probing each beam separately with the point of a sewing needle (#10 sharp) and measuring the resultant scattered light detected by the photomultiplier tube. The needle will be placed at the edge of the beam in the region of the He-Ne beam focal location with the point protruding into the beam. The needle will traverse the beam perpendicular to the longitudinal axis. Scattered light signal measurements will be recorded by the dedicated personal computer. The data will be used to confirm the calculated beam waists and to ensure that the beams are concentric.

In step two, precision pinholes of known diameters ranging from 5 μm to 150 μm located at the He-Ne beam focal location act as scattering objects and allow correlation of pinhole size with the intensity of the measured light signal.

Step three of the calibration utilizes a Berglund-Liu vibrating orifice aerosol generator (TSI model 3450) to produce monodispersed particles of known diameter. The particles pass through the focal volume of the two laser beams. Scattered light signals as a function of known droplet size will be compared to the pinhole data and the final correlation between particle size and scattered light intensity will be produced.

Signal Conditioning

The primary requirement of the signal conditioning subsystem for the forward-scatter channel is to allow acquisition of rapid transients where the dynamic range of the signal is approximately three orders-of-magnitude. This 1000:1 variation in signal level is a result of the large difference in the light scattered by the smallest and largest anticipated droplets.

Based on estimates of droplet velocities, the system frequency response must extend to approximately 40 kHz. This combination of large dynamic range and wide bandwidth frequency response presents a challenge if high signal-to-noise ratios are to be obtained.

Table 1 illustrates the solution to the signal conditioning and data acquisition problem. (See also Fig. 2). The signal from the forward-scatter PMT is amplified by a PARC (model 181) preamplifier which provides flat response up to 100 kHz. The noise floor of the amplifier is below that of the dark current noise from the PMT. A buffer impedance-matching amplifier, designed and fabricated in-house, is used to interface between the 1kΩ impedance of the preamplifier and the 50Ω impedance input to the logarithmic amplifier (Analog Modules model 381). The log amplifier compresses the

TABLE 1

Electronic Components for the Forward-Scatter Channel

Parameter \ Component	1P28A PMT	PARC Model 181 Preamp	Buffer	Analog Modules Model 381 Log Amp	Rapid Systems R2040 A/D
Noise (dark current)	2-10 nA	0.02-0.1 mV	—	~ 0 V	~ 0 V
Minimum Signal	100 nA	1.0 mV	1.0 mV	0.17 V	0.17 V
Maximum Signal	100 mA	1.0 V	1.0 V	0.64 V	0.64 V
Input Impedance	—	variable	400 kΩ	50 Ω	1 MΩ
Output Impedance	current source	1 kΩ	6 Ω	50 Ω	—
Bandwidth	—	100 kHz	>100 kHz	80 MHz	20 M sample/s

1mV to 1V input range to an output range of 0.17 to 0.64 V. This compression is necessary to accommodate the 8-bit resolution of the A/D data acquisition system, i.e. a dynamic range of 10^3 would require a resolution of 1 part in 10,000 (for 10% accuracy), while 8-bits provides only 1 part in 256.

For the signal validation channel (He-Ne laser scattering signal), the frequency requirement is more stringent while the dynamic range is relaxed in comparison to the forward-scatter channel. The increased frequency response requirement is a result of the He-Ne scattering pulse being much more narrow than the forward-scattered light pulse. The relaxation of the dynamic range requirement is a result of not needing a quantitative measure of the signal level, but merely an indication of the pulse shape. Furthermore, the narrow width of the focused He-Ne beam results in less variation in scattering intensity when the size of the scattering centers (droplets) equals or exceeds the beam width. A current amplifier (Analog Modules model 341-B) with a bandwidth of DC to 1.5 MHz and a gain of 1 MV/A provides an output signal readily acquired by the A/D board. An identical current amplifier conditions the signal from the PMT used to detect ignition of the aluminum.

Data Acquisition and Processing

The primary function of the data acquisition system is to collect data from the three photomultipler channels. Three additional data channels have been included to collect information such as laser power and thermocouple voltages.

As a particle passes through the focal volume of the laser system the scattered laser light will generate a pulse-like signal in the PMT output voltages on the He-Ne and Ar-ion channels. The intensity of the signal on the Ar-ion channel will be used to determine the particle size and the peak width will be used to calculate the particle velocity. This data will be valid only if the particle passes near the center of the Ar-ion beam. To confirm this, the He-Ne channel output will be checked for a peak occuring at

the same time as the peak on the Ar-ion channel. If this is not the case, the signals must be rejected.

Particle transit times through the beams are estimated to be on the order of 16-160 μs for the He-Ne beam and 70-700 μs for the Ar-ion beam. A two-channel, 20 MHz A/D data acquisition board (Rapid Systems, Inc. model R2040) was selected for data collection from the two laser channels. For example, the high sampling rate of this board will provide 320 sample points on the He-Ne channel signal for a 5 m/s post-flame flow rate, giving excellent time resolution of the signal.

The data provided by the ignition channel will be used to determine whether a particle has ignited or not. This requires only the detection of the signal, not the signal shape. Based on this requirement, a four-channel, 500 KHz board (Rapid Systems Inc., model R1040) was selected for the ignition and auxilliary data channels. Both the R2040 and R1040 boards are connected to a dedicated AT&T model 3600 personal computer.

These two A/D boards have both pre-trigger and post-trigger data buffers, permitting the use of any point on one of the channel inputs as a signal to start the data collection. For measurements of a particle to be valid, the particle must generate a signal on the He-Ne channel as described above. Therefore, this channel will be used as the trigger channel, providing the first step in the signal validation process.

After triggering and filling the A/D buffer, the computer handles the data validation and collection process. The computer program written for these tasks consists of a main menu control, data acquisition commands and data analysis. The menu section provides set-up of the acquisition parameters for both boards and a choice of either data collection or analysis.

The data collection part of this program performs the signal validation and records the pulse height and width of the Ar-ion signal and whether or not the particle

was ignited. Data from the auxilliary channels are stored in a user-specified file for later analysis. Important board operating parameters and user comments are also written to this file.

Signal validation involves checking for the presence of multiple particles in the probe volume, peak saturation, pulse shape, and whether the Ar-ion pulse is completely contained within the data sample taken. The program will only accept complete single particle signals for analysis, rejecting all other data. The peak and the leading and trailing edges of the Ar-ion signal also are located at this time. The Ar-ion signal pulse width is then calculated, and the pertinent information is passed to storage. This extraction of the critical information from the signal drastically reduces the disk space required to define a single particle, making possible the storage of a large number of samples.

The data analysis portion of this program reads particle data from a specified file and performs the necessary sizing and velocity calculations based on drop-size calibrations of the laser system. After this is done, the results are written to a second data file for further statistical and graphical analysis.

The first section of the code has been completed and debugged, and work has begun on the data collection portion of the program. There were some initial problems implementing the vendor-supplied software, originally written to handle only one acquisition board, with the two boards being used. With help from the vendor, the problems were solved.

BURNER AND SPRAY RIG

The design objectives for the burner and spray rig are:

1. Provide a laminar, homogeneous post-flame region for slurry ignition;
2. Allow flashback-free operation over a range of stoichiometries while operating with oxidizers ranging from air to 100% oxygen;

3. Isolate the post-flame gases from the ambient atmosphere;

4. Produce a spray of aluminum slurry droplets varying in size from approximately 10 to 100 μm in diameter and introduce this spray into the post flame region;

5. Provide for fixed mounting of laser optics through the use of a traversing burner support.

Burner Design

Based upon the above objectives, a non-premixed burner was designed and fabricated following the basic design outlined in Ref. [8]. The burner is shown schematically in Fig. 3. The gaseous fuel enters the base of the burner and passes through a dispersion ring that evenly distributes the gas around the perimeter of a fuel chamber. From here, the fuel passes through 72 17-gauge (1.04 mm i.d.) stainless steel tubes and exits the burner at the top surface of the honeycomb matrix. The oxidizing gas enters the middle section of the burner and passes through another dispersion ring above the manifold plate. This gas then flows up around the 72 fuel tubes and through the open cells of the honeycomb matrix surrounding these tubes. This configuration results in a small, laminar, diffusion flame at the exit of each fuel tube. These flames merge within 5 to 10 mm of the burner surface [8], providing an excellent approximation of a pre-mixed, laminar, flat flame. Slurry droplets are generated in the spray chamber at the bottom of the burner and then pass through a 13-gauge (1.8 mm i.d.) tube located along the centerline of the burner, emerging in the center of the burner face.

Operating under rich conditions requires that the flame region be isolated from the ambient air to prevent the diffusion of ambient oxygen to the product gases. This

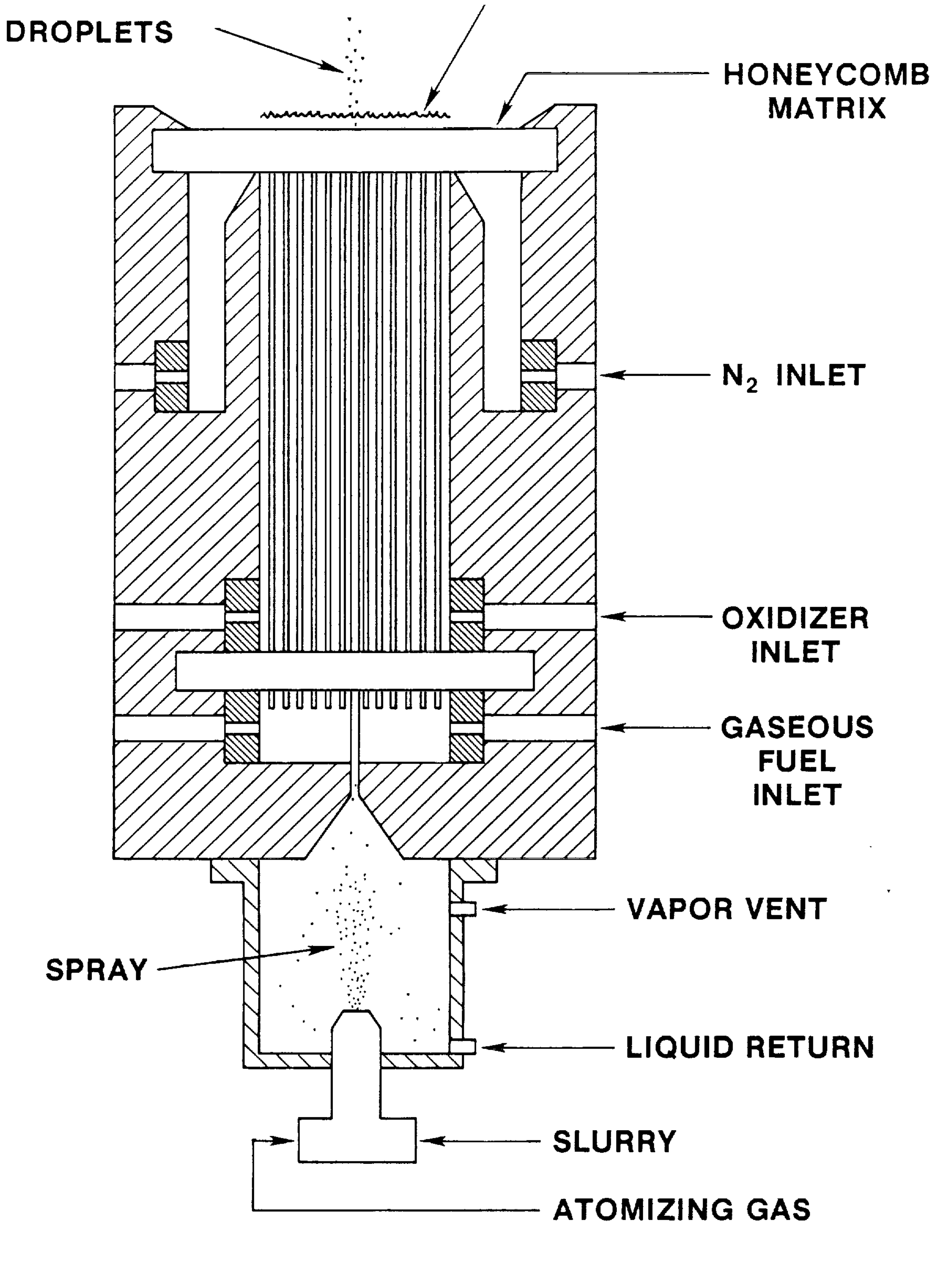

FIGURE 3. Schematic diagram of burner and spray generator.

oxygen would react with the rich products causing a secondary, conical flame above the burner surface. This is avoided by placing a curtain, or shroud, of nitrogen around the flame that prevents the post-flame gases from mixing with the surrounding air. Lean mixtures do not present this problem since excess oxygen is already present in the product gases.

The present burner design offers several advantages over conventional laminar flat-flame burners. Since the fuel and oxidizer gases do not mix until they reach the flame, flashback and flammability limits are not a problem. In addition, cooling of the burner head is provided by the flowing reactants, eliminating the need for water cooling, and providing a highly adiabatic flame.

Using ignition data from previous work [4], approximate ignition times were extrapolated for the range of particle sizes under study. From this data, it was found that all of the particles should ignite within 24 cm, given a post-flame gas velocity of 5 m/s. With propane as a fuel, post-flame velocities ranging from 4.6-57.5 m/s can be expected based on mixture flame speeds and volume expansion ratios of 9.7 to 15.5. Combining this information with expected gas consumption rates for various size burners, a burner diameter of 7 cm was decided upon. For a laminar flame, this yields a homogeneous region extending to a height of approximately 21 cm. Based on the work of R. S. Barlow et. al. [8], a 3 cm wide annular nitrogen shroud was designed into the burner head to isolate the post-flame region from the ambient air.

Current plans call for this burner to be used with several different fuels and a wide range of oxygen concentrations to provide a variety of conditions for slurry combustion. In addition, the fuel tubes must be small enough to produce laminar flow, but large enough to prevent soot clogging. The oxidant flow velocity should be approximately equal to that of the fuel, but as long as a laminar oxidant flow is maintained, the flame remains laminar and efficient mixing of the fuel and oxidant occurs [9].

With these constraints in mind, the burner head was designed. A 403 stainless steel honeycomb matrix with a 1.6 mm cell diameter was used to position the fuel tubes and to straighten the oxidizer flow. A fuel tube pattern, in which the tubes are separated from each other by one open honeycomb cell in all directions, was decided upon. This results in each of the small flames being surrounded by flowing oxidizer, yet keeps the flames close enough to each other such that they rapidly merge.

The burner was fabricated, assembled, and tested for leakage between the fuel manifold and the oxidant chamber. After this testing, the burner was operated using a methane-oxygen flame. The burner appeared to be functioning correctly during this time, but a leak developed in the manifold plate between the fuel and oxidizer chambers, creating a flame underneath the honeycomb matrix that melted the honeycomb and some of the fuel tubes. Additional honeycomb material was ordered, and the burner should be ready for re-assembly by early January, at which time a better seal will be employed, and a more demanding seal test will be performed.

Translation System

It is desirable to provide for fixed mounting of the laser optics, where alignment and vibration are critical, while allowing the burner to translate. Presently, a support system for the burner is being constructed using optical mountings to provide a high degree of accuracy in positioning the burner. Three-dimensional translation is provided by the use of two horizontal positioners and one optical jack mounted on a metal frame, which in turn, is bolted to the floor. This system allows for a vertical translation of 7.6 cm, and a horizontal translation in both the X and Y directions of approximately 5.1 cm. Additional vertical travel ranges can be provided by adjusting the metal frame or by the addition of another jack.

This system will allow the atomizer feed tube to be positioned at the focal point of the laser system once it is aligned, ensuring an accurate alignment of the burner and the

laser system. A method of measuring the burner elevation with respect to the laser system is being designed, together with a mounting system for the Bergund-Liu droplet generator, which will be used in the drop size calibration process.

Slurry Atomizing System

The atomizing system must provide slurry droplets ranging in size from approximately 10 to 100 microns. In addition, the system must also allow drainage of excess slurry from the atomizing chamber, control of the droplet velocity entering the flame, and control of the stoichiometry of the atomizing gas.

The atomizing nozzle was selected based on work with coal/water slurries [10]; and because of possible atomizing differences, bench tests were performed with aluminum slurry samples. The bench tests were performed on a Spraying Systems Co. conical atomizing nozzle, set-up number 12A, identical to the one used in the coal/water research [10], and four different diameter slurry feed tubes ranging in size from 1.6 to 6 mm.

The nozzle was mounted at the base of a cylindrical plexiglas chamber. A needle valve was mounted on the side of the chamber to bleed off excess gas, allowing control of the droplet velocity in the slurry feed tube mounted at the top of the chamber. A flexible plasticene seal was used around the feed tube to permit adjustment of the distance between the nozzle and the tube entrance. The system was tested using the different feed tube diameters both with and without a funnel shaped tube entry region. A He-Ne laser was used to illuminate the droplets exiting from the feed tube. Nitrogen was used as the atomizing gas and the slurry was injected into the nozzle by a syringe pump.

On a qualitative basis, it was found that the conical shield aided the slurry flow through the tube, that a 2.4 millimeter diameter tube provided the best droplet flow, and that this system worked best when the tube entrance was placed approximately 10.1 to 12.7 cm above the nozzle. These operating conditions produced a steady stream of

atomized droplets exiting from the droplet tube with virtually no clogging. Ideal flow rates for both the slurry and the gas will be determined during the system shakedown process.

During actual operation with the burner, the slurry will be fed to the atomizing nozzle by a syringe pump, and the atomizing gas will be a mixture of nitrogen and oxygen, with selected oxygen concentrations to match the desired operating conditions in the post-flame region. Excess slurry will be drained off by a vacuum sump, preventing slurry accumulation in the bottom of the atomizing chamber that might adversely affect the atomization process. In addition, a gas bleed valve will be mounted on the chamber, allowing control of the flow velocity through the droplet tube. This system has been fabricated, but has yet to be tested. Shakedown of this system will be accomplished following that of the burner.

FUTURE PLANS

During the next 6-month period the following activities are planned:

1. Reassembly of the burner with new honeycomb and fuel tubes and leak testing.
2. Operation of the burner and spray rig with a pure liquid fuel and subsequently with an aluminum slurry.
3. Calibration of flow measuring devices for all gases and slurry flows.
4. Shakedown of the optical and electronics systems.
5. Calibration of the particle sizing system with (1) pinholes and (2) free droplets from a Berglund-Liu droplet generator.
6. Completion of software development for data acquisition and signal processing.
7. Integrated operation of the complete system (burner, spray rig, particle sizing and velocimetry systems, data acquisition, and data processing) using pure liquids and aluminum slurry fuels.
8. Perform screening study to establish which slurry formulation should be used as a baseline.
9. Begin parametric study using baseline slurry.

REFERENCES

1. Faeth, G. M., "Status of Boron Combustion Research," CPIA Pub. 412, Vol. I, pp. 15-29, 1984.

2. Rapp, D. C., and Zurawski, R. L., "Characterization of Aluminum/RP-1 Gel Propellant Properties," AIAA paper AIAA-88-2821 presented at the AIAA/ASME/SAE/ASEE 24th Joint Propulsion Conference, July 11-13, 1987.

3. Zurawski, R. L., "Current Evaluation of the Tripropellant Concept," NASA Technical Paper 2602, 1986.

4. Wong, S.-C., and Turns, S. R., "Ignition of Aluminum Slurry Droplets," Combustion Science and Technology, 52:221-242, 1987.

5. Turns, S. R., Wong, S.-C., and Ryba, E., "Combustion of Aluminum-Based Slurry Agglomerates," Combustion Science and Technology, 54:299-318.

6. Holve, D. J., Tichenor, D., Wang, J. C. F., and Hardesty, D. R., "Design Criteria and Recent Developments of Optical Single Particle Counters for Fossil Fuel Systems," Opt. Engrg., 20:529-539, 1981.

7. Wang, J. C. F., and Hencken, K. R., "In Situ Particle Size Measurements Using a Two-Color Laser Scattering Technique," Applied Optics, 25:653-657, 1986.

8. Barlow, R. S., Dibble, R. W., Chen, J.-Y., and Lucht, R. P., "Effect of Damkohler Number on Superequilibrium OH Concentration in Turbulent Nonpremixed Jet Flames," AIAA paper AIAA-89-0061 presented at the 27th Aerospace Sciences Meeting, January 9-12, 1989.

9. Krupa, R. J., Culbreth, T. F., Smith, B. W., and Winefordner, J. D., "A Flashback-Resistant Burner for Combustion Diagnostics and Analytical Spectromety," Applied Spectroscopy, 40:729-733, 1986.

10. Holve, D. J., and Meyer, P. L., "Coal/Water Slurries: Fuel Preparation Effects on Atomization and Combustion," Combustion Science and Technology, 52:243-268, 1987.